

NJC

Accepted Manuscript



This is an *Accepted Manuscript*, which has been through the Royal Society of Chemistry peer review process and has been accepted for publication.

Accepted Manuscripts are published online shortly after acceptance, before technical editing, formatting and proof reading. Using this free service, authors can make their results available to the community, in citable form, before we publish the edited article. We will replace this *Accepted Manuscript* with the edited and formatted *Advance Article* as soon as it is available.

You can find more information about *Accepted Manuscripts* in the [Information for Authors](#).

Please note that technical editing may introduce minor changes to the text and/or graphics, which may alter content. The journal's standard [Terms & Conditions](#) and the [Ethical guidelines](#) still apply. In no event shall the Royal Society of Chemistry be held responsible for any errors or omissions in this *Accepted Manuscript* or any consequences arising from the use of any information it contains.



www.rsc.org/njc

Novel organic–inorganic hybrid soft xerogels with lanthanide complexes through an ionic liquid linkage

Cite this: DOI: 10.1039/x0xx00000x

Zhi-Yuan Yan, Bing Yan*

Received 00th January 201x,
Accepted 00th January 201x

DOI: 10.1039/x0xx00000x

www.rsc.org/

This paper provides the strategy to prepare luminescent sandwich structured hybrid materials $[\text{Ln}(\text{L})_4] \text{IM}^+-\text{Al}/\text{Ti}$ ($\text{Ln} = \text{Eu}, \text{Sm}$; $\text{L} = 2\text{-thenoyltrifluoroacetate (TTA)}$; $\text{Ln} = \text{Tb}$, $\text{L} = \text{trifluoroacetylacetone (TAA)}$) based with sol-gel derived hosts of Ti-O or Al-O networks. The ionic liquid compound 3-(2-carboxyethyl)-1-methylimidazolium bromide (IM^+Br^-) plays double roles of both connecting lanthanide compounds with ion exchange reaction and linking matrices through its carboxylic group. Subsequently, series of hybrid soft materials of alumina and titania xerogels centered with lanthanide complexes are prepared via hydrolysis and polycondensation of aluminum isopropoxide or tetrabutyl titanate. These hybrid soft xerogels are characterized under FTIR, XRD, UV–VIS diffuse reflection absorption spectra, SEM, TGA and especially luminescence spectroscopy. The results prove that it is an effective way to prepare $[\text{Ln}(\text{L})_4] \text{IM}^+-\text{Al}/\text{Ti}$ hybrid soft materials with favorable photoluminescent behaviors. It is noticeable that $[\text{Sm}(\text{TTA})_4] \text{IM}^+-\text{Ti}$ can render white light under broadband excitation for certain content of Sm^{3+} .

Introduction

Lanthanides complexes have been playing a special role as new functional materials in photonic applications for many practical fields including phosphor¹, solid-laser device² and optical amplifier³, *etc.* Based on the effective energy transfer between ligands and luminescent central lanthanide ions, lanthanides complexes own characteristic luminescence with sharp, intense emission lines under ultraviolet light irradiation for parity and spin-forbidden 4f–4f transitions⁴. Owing to the direct photo-excitation of Ln^{3+} is not effective to limit the light output, we choose organic ligands⁵ (heterocyclic ligands, calixarenes and aromatic carboxylic acids), whose organic chromophores are strongly bonded to Ln^{3+} centers covering from ultraviolet (Ce^{3+} and Gd^{3+}) to the near-infrared regions (Nd^{3+} , Er^{3+} , Tm^{3+} and Yb^{3+})⁶. Furthermore, lanthanides complexes based hybrid materials have attracted a great amount of attention due to their extraordinary properties, which exhibit exceptional properties exceeding what would be expected for materials with simple components⁷. They generate simultaneously controllable red, green and blue (RGB) emissions, achieving white-light simulation⁸. And they combine good mechanical, thermal, and chemical stability, whether exposed to the homoeothermic air or in a confined high temperature environment⁹.

Recently, there is increasing attention about room-temperature ionic liquids (IL) as a convenient media applied in organic synthesis and separation⁹, which possess very low vapor pressure, good electric conductivity and less toxicity than most organic solvents¹⁰, especially for metal-containing ionic liquids gathering lots of interest¹¹. Binnemans and his co-workers have reported series of research about task-specified ionic liquid (TSIL) bearing a carboxyl group to dissolve metal oxides¹². The current research of our group is focused on the ionic liquid bridge to construct derived functional materials that lanthanide complexes are linked with ionic liquids by electrostatic forces¹³. Our aim is to explore the possibility of imidazolium salts with a carboxyl group to assemble photofunctional materials¹⁴, which provides a new path to construct luminescent hybrids with double functional linker of both ionic and covalent

interaction¹⁵. According to the recently literature¹⁶, there are few reports on the dual use of ionic liquids, which introduce the lanthanide β -diketonate complex into Al-O or Ti-O matrices.

Herein, the design and construction of lanthanide organic-inorganic hybrid soft xerogel materials $[\text{Ln}(\text{L})_4] \text{IM}^+-\text{Al}/\text{Ti}$ ($\text{Ln} = \text{Eu}, \text{Tb}, \text{Sm}$; $\text{L} = \text{TTA}$ and TAA) have been accomplished using sol-gel method. It is worth mentioning that $[\text{Sm}(\text{TTA})_4] \text{IM}^+-\text{Ti}$ can fall in the white light region under a relatively wide wavelength excitation, which has potential as novel optical materials.

Experimental section

Materials

The lanthanide oxides were all with purity of Eu_2O_3 (99.9 %), Tb_4O_7 (99.9 %) and Sm_2O_3 (99.9 %). $\text{RECl}_3 \cdot x\text{H}_2\text{O}$ were synthesized by dissolving corresponding lanthanide oxides in hydrochloride solution and dried up after filtration and washing with ice deionized water and diethyl ether for several times. 1-Methylimidazole (99 %, Aladdin), oleic acid (OA, 90 %, Alfa Aesar), aluminum isopropoxide and tetrabutyl titanate (99 %, Aladdin) were distilled and stored under nitrogen atmosphere. 3-bromopropanoic acid (98 %), ferric chloride ($\text{FeCl}_3 \cdot 6\text{H}_2\text{O}$), ferrous chloride ($\text{FeCl}_2 \cdot 4\text{H}_2\text{O}$), thenoyltrifluoroacetone (TTA, 98 %), trifluoroacetylacetone (TAA, 98 %) and cetyltrimethylammonium bromide (CTAB) were purchased from Aldrich and used as received.

Synthetic procedures

Synthesis procedure of 3-(2-carboxy-propyl)-1-methylimidazolium bromide (IM^+Br^-)

According to previous literature reporting¹⁷, the synthesis of the ionic liquid - IM^+Br^- is a comparatively easy task as following: equal molar amounts 3-bromopropanoic acid and 1-methylimidazole (0.1 mol) was put together in a round-bottom flask under magnetic stirring in argon atmosphere. Then the mixture was refluxed at 80 °C for 7 hrs. Ethyl acetate was used to clean unwanted substances in ionic liquid. Then the ionic liquid product was obtained by evaporation of the solvent under vacuum at 60 °C. After final cleaning, transparent and viscous liquid was obtained. ¹HNMR

(400MHz, DMSO): 9.21(d, 1H, $^3J=5.6\text{Hz}$), 7.74(t, 2H, $^3J=5.6\text{Hz}$), 4.36(t, 2H, $^3J=4\text{Hz}$), 3.86(s, 3H, $^3J=19.2\text{Hz}$), 3.18(t, 2H, $^3J=9.8\text{Hz}$)

Preparation of anionic lanthanide (III) tetrakis(β -diketonate) complexes denoted as $\text{Ln}(\text{L})_4$ ($\text{Ln} = \text{Eu, Tb, Sm}$; $\text{L} = \text{TTA}$ and TAA):

Taking $[\text{Eu}(\text{TTA})_4]^-$ as an example, lanthanide complexes were synthesized according to modified literature procedure¹⁸. TTA and NaOH (1: 1 molar ratio) were dissolved in a certain amount of absolute ethanol. The reaction temperature was maintained at 60 °C for about 5 hrs. Then an appropriate amount of $\text{EuCl}_3 \cdot 6\text{H}_2\text{O}$ ethanol solution was added into the above mixed solution by stirring at 60 °C for 2 hrs (the molar ratio of TTA: $\text{Eu}^{3+} = 4: 1$). After the removal of the precipitates by filtration, the supernatant was concentrated using a rotary vacuum evaporator, resulting in the products.

Synthesis of lanthanide functionalized through sol-gel-derived hybrid materials $[\text{Ln}(\text{L})_4]^- \text{IM}^+ \text{-Al/Ti}$ ($\text{Ln} = \text{Eu, Tb, Sm}$; $\text{L} = \text{TTA}$ and TAA)

Firstly, the prepared lanthanide (III) tetrakis(β -diketonate) complexes and IM^+Br^- (the molar ratio 1: 1.5) were put in ethanol solution. After stirring constantly at 50 °C for 2 days, ions exchange reaction reaches fully complete. The resulting materials were prepared by centrifugation and extensive washing with ethanol to remove excess ionic liquid and other substances. The elemental analyses data (wt %): Anal. (Calcd.) for $[\text{Eu}(\text{TTA})_4]^- \text{IM}^+$: Eu, 12.90 (12.76); C 39.52 (39.34); H 2.06 (2.20); N 2.19 (2.35). Anal. (Calcd.) for $[\text{Tb}(\text{TAA})_4]^- \text{IM}^+$: Tb, 17.31 (17.17); C 34.88 (35.04); H 2.69 (2.83); N 2.92 (3.03). Anal. (Calcd.) for $[\text{Sm}(\text{TTA})_4]^- \text{IM}^+$: Sm, 12.77 (12.64); C 39.53 (39.39); H 2.05 (2.20); N 2.19 (2.36). Then, adding aluminum isopropoxide / titanium tetrabutoxide (the molar ratio of Ln^{3+} : Al/Ti = 1: 10, 1: 40) into the above solution, keeping the hydrolysis reactions via reflux condenser. Lastly, to wash the product with ethanol and remove solvent by vacuum rotary evaporation at 50 °C, the final product was obtained after vacuum dried. It is worth mentioning that $[\text{Ln}(\text{L})_4]^- \text{IM}^+ \text{-Al}$ is white powder and the latter is yellow gel. These soft hybrid materials were named as $[\text{Ln}(\text{L})_4]^- \text{IM}^+ \text{-Al}$, $[\text{Eu}(\text{TTA})_4]^- \text{IM}^+ \text{-Ti1}$, $[\text{Eu}(\text{TTA})_4]^- \text{IM}^+ \text{-Ti2}$ ($\text{Ln} = \text{Eu, Tb, L} = \text{TTA}$; $\text{Ln} = \text{Sm, L} = \text{TAA}$; Ti1, Ln: Ti = 1: 10; Ti2, Ln: Ti = 1: 40)

Physical measurements

Fourier transform infrared (FTIR) spectra are measured within the 4000-400 cm^{-1} region on a Nexus 912 AO446 spectrophotometer with the KBr pellet technique. Elemental analysis is carried out by an Elementar Carlo EL elemental analyzer. The X-ray powder diffraction patterns (XRD) are recorded on a Bruker D8 diffractometer (40 mA-40 kV) using monochromated Cu K α radiation ($k = 1.54 \text{ \AA}$) over the 2θ range of 10-80 °. Field emission scanning electronic microscope (SEM) images are obtained with a Philips XL-30. Luminescence spectra measurements (using a 450 W xenon lamp as the excitation source) are carried out on an Edinburgh Instruments FLS-920 phosphorimeter. Thermogravimetric analyses (TG and DTG) are carried out using a Netzsch STA 449C system at a heating rate of 5 °C/min under the nitrogen protection. The diffuse reflectance UV-Vis spectra of the powdered samples are recorded by a BWS003 spectrophotometer.

Results and discussion

Figure 1 shows the scheme for the synthesis and basic composition of whole hybrid systems. As shown in Figure 1(a), $\text{Ln}(\text{III})$ tetrakis β -diketonates complexes are introduced to replace Br^- of the above system, resulting in the hybrid system by the static electric interaction of the positive (IM^+) and negative charge ($[\text{Ln}(\beta\text{-diketonate})_4]^-$). On the other hand, the IM^+ fragment can link alumina and titania xerogel matrices through the coordination interaction between its carboxylic groups and Al^{3+} or Ti^{4+} . So the liquid compound behaves as the double functional linker to connect lanthanide complexes and xerogels, just like sandwich mode (See Figure 1(b)). Figure 1(c) presents the selected photograph of the final xerogels of $[\text{Ln}(\text{L})_4]^- \text{IM}^+ \text{-Ti}$ hybrids, revealing the formation of transparent and stable xerogel forms.

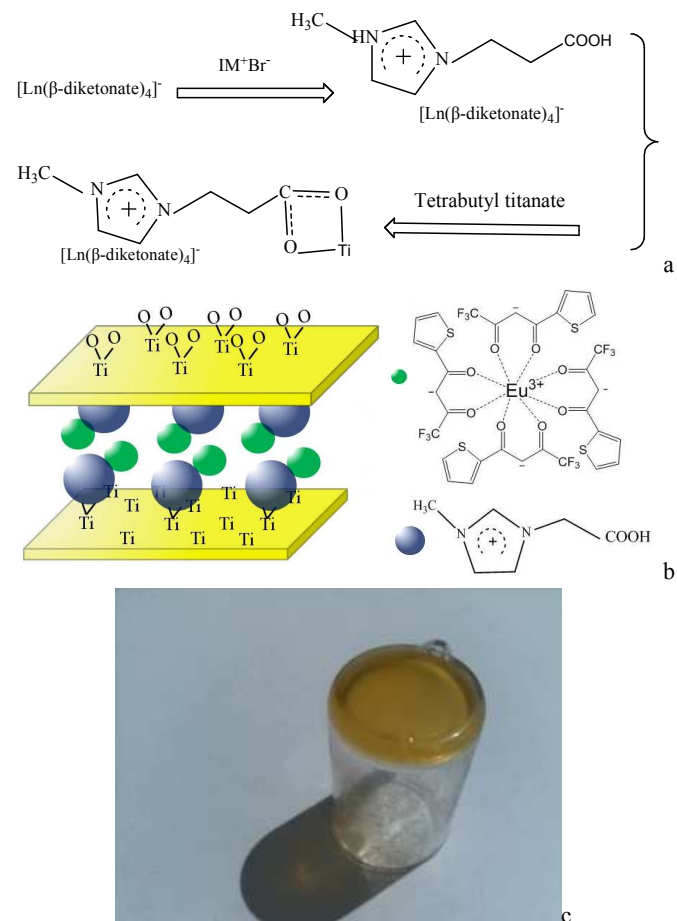


Figure 1 The fabrication scheme of the synthesis process of hybrid soft xerogel material $[\text{Eu}(\text{L})_4]^- \text{IM}^+ \text{-Ti}$: (a) the scheme for synthesis, (b) the scheme for sandwich composition and structure; (c) the photograph for soft gels $[\text{Ln}(\text{L})_4]^- \text{IM}^+ \text{-Ti1}$. Here we only set $[\text{Eu}(\text{TTA})_4]^- \text{IM}^+ \text{-Ti}$ as an example, and for other $[\text{Ln}(\text{L})_4]^- \text{IM}^+ \text{-Ti}$ ($\text{Ln} = \text{Eu, Tb, Sm}$; $\text{L} = \text{TTA}$ or TAA) systems, the scheme is similar except for Eu is replaced by Tb or Sm, TTA is replaced by TAA and titania (Ti) is replaced by alumina (Al).

Figure 2 (a) displays the IR spectra of $[\text{Ln}(\text{L})_4]^- \text{IM}^+ \text{-Al}$ ($\text{Ln} = \text{Eu, Tb, Sm}$), the typical antisymmetric and symmetric stretching vibrations of carboxylate appear at about 1575 and 1455 cm^{-1} , indicating that the carboxylic acid substituted ionic compound IM^+ was completely reacted with titania or alumina and no dissolution occurred during the sol-gel procedure¹⁹. Originally, the absorption

band of C=O should appear at about 1720 cm^{-1} from IM^+ , upon the reaction with aluminum isopropoxide, the stretching vibration of C=O of COOH groups disappear. Meanwhile the bands at 1166 cm^{-1} vibration still exists, ascribed to $\nu_{\text{C-O}}$, which proves that the carboxyl groups on the ion liquid involved in the reaction. Because of the delocalization presence of C-O-Al bonds in the $[\text{Ln}(\text{L})_4]\text{IM}^+\text{-Al}$ materials, wherefore the absorption bands at 1072 cm^{-1} and 622 cm^{-1} can be ascribed to $\nu_{\text{C-O}}$ and $\nu_{\text{Al-O}}$. What is worth mentioning, the absorption band at approximately 498 cm^{-1} both emerges in $[\text{Ln}(\text{L})_4]\text{IM}^+\text{-Al}$ and $[\text{Ln}(\text{L})_4]\text{IM}^+\text{-Ti}$, due to $\nu_{\text{Ln-O}}$, which is further evidence of successful connection between lanthanides and ligands. From Figure 2(b) for $[\text{Ln}(\text{L})_4]\text{IM}^+\text{-Ti1}$ (Eu, Tb, Sm), we can see immediately that there are similar characteristic absorption bands at 1572 cm^{-1} and 1441 cm^{-1} , which should be ascribed to the antisymmetric and symmetric stretching vibrations of carboxylate¹⁸. Likewise, the absorption bands appearing at 1166 cm^{-1} is ascribed to $\nu_{\text{C-O}}$ of COOH group, With the disappearance of characteristic peak of $\nu_{\text{C=O}}$ of COOH group (center at about 1720 cm^{-1}), whereas the absorption bands arising at 1088 cm^{-1} and 802 cm^{-1} can be affected by the delocalization caused from $\nu_{\text{C-O}}$ and $\nu_{\text{Ti-O}}$. In addition, the absorption bands at about 3400 cm^{-1} is assigned to the O-H stretching vibration of the remind water cannot be prohibited for all materials. Therefore, all the emerging absorption peaks which we have discussed above suggest that the lanthanide complexes functionalized devised xerogel material have been achieved.

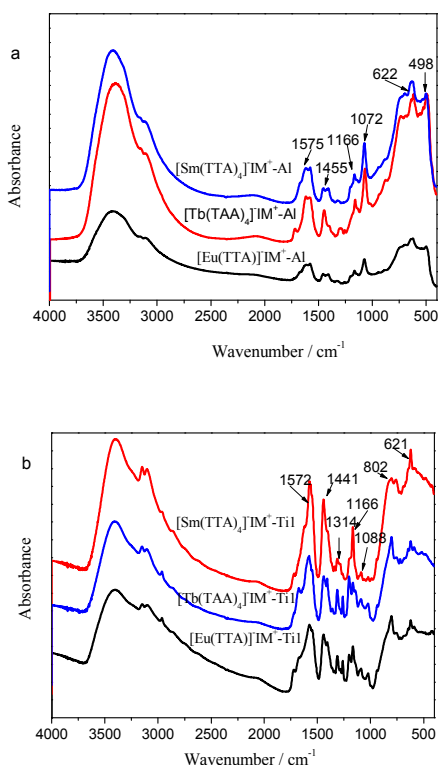


Figure 2 FTIR spectra of hybrid xerogels: (a) $[\text{Ln}(\text{L})_4]\text{IM}^+\text{-Al}$, (b) $[\text{Ln}(\text{L})_4]\text{IM}^+\text{-Ti1}$ (Ln = Eu, Tb, Sm; L = TTA or TAA).

The selected room temperature X-ray diffraction (XRD) patterns of $[\text{Ln}(\text{L})_4]\text{IM}^+\text{-Al}$ and $[\text{Ln}(\text{L})_4]\text{IM}^+\text{-Ti}$ (Ln = Eu, Tb, Sm, L = TTA, TAA) are shown respectively in Figure S1 (a) and (b) from 10° to

80° . According to Figure S1(a), (b), they may be probably coming from Al-O network and Ti-O network respectively. Comparing with the two figures, $[\text{Ln}(\text{L})_4]\text{IM}^+\text{-Al}$ hybrids show better crystallization than $[\text{Ln}(\text{L})_4]\text{IM}^+\text{-Ti1}$ systems, well consistent with the state of the product obtained. $[\text{Ln}(\text{L})_4]\text{IM}^+\text{-Al}$ hybrids present typical boehmite crystal structure, showing the crystallization is nearly complete to form boehmite²⁰. In addition, as we know, lanthanides have similar radius, coordination environment and physical and chemical nature, so the XRD patterns of different lanthanide s (Eu^{3+} , Tb^{3+} , Sm^{3+}) hybrid materials have almost no difference.

The UV-Vis diffuse reflectance spectra measurements are performed on all the solid materials, which are shown in Figure S2. It can be seen that all the spectra exhibit the similar broad absorption band in the UV-Vis range (240-500 nm), which are mainly attributed to the absorption of the β -diketone ligands (TTA or TAA), no matter containing different lanthanides materials. These adsorption bands also partially overlap with the photoluminescence excitation spectra respectively. The organic ligands can sensitize the emission of lanthanide ions via intramolecular energy transfer when absorbing the ultraviolet light. In particular, the peaks at 614 nm and 545 nm can be observed in the spectra of $[\text{Eu}(\text{TTA})_4]\text{IM}^+\text{-Al}$ (Figure S2(a)) and $[\text{Tb}(\text{TAA})_4]\text{IM}^+\text{-Al}$ (Figure S2(b)) hybrids, which is due to the corresponding Eu^{3+} and Tb^{3+} ion, respectively. Accordingly, it can be speculated that an effective energy transfer exists between TTA and $\text{Eu}^{3+}/\text{Sm}^{3+}$ or TAA and Tb^{3+} within these hybrid systems. That is can be proved by the following photoluminescence property.

Figure S3 compares the selected SEM images of the hybrid materials $[\text{Eu}(\text{TTA})_4]\text{IM}^+\text{-Al}$ and $[\text{Eu}(\text{TTA})_4]\text{IM}^+\text{-Ti1}$. The former appears to be homogeneous and uniform particles with the size approximately 1-2 μm , which may be caused a lot of Al-O groups forming the aluminum oxide network. On the other hand, the soft xerogel material $[\text{Ln}(\text{TTA})_4]\text{IM}^+\text{-Ti1}$ varies differently compared with $[\text{Eu}(\text{TTA})_4]\text{IM}^+\text{-Al}$, which can be attributed to the formation of titanyl network with excessive fast speed.

To investigate the thermal stability of the obtained hybrid materials, the thermogravimetric (TG) and the corresponding derivative weight loss (DTG) analysis have been performed for $[\text{Ln}(\text{L})_4]\text{IM}^+\text{-Al}$ and $[\text{Ln}(\text{L})_4]\text{IM}^+\text{-Ti}$. Figure S4 shows the selected TG and DTG curves of $[\text{Eu}(\text{TTA})_4]\text{IM}^+\text{-Al}$ and $[\text{Eu}(\text{TTA})_4]\text{IM}^+\text{-Ti1}$ hybrids, at a heating rate of $5^\circ\text{C}/\text{min}$ under nitrogen atmosphere. Three main degradation steps can be observed, the first step of mass is about 9 % for $[\text{Eu}(\text{TTA})_4]\text{IM}^+\text{-Al}$ and $[\text{Eu}(\text{TTA})_4]\text{IM}^+\text{-Ti1}$ from 30 to 190°C may be due to the desorption of physically adsorbed water and residual water or other solvent, combining with the DTG analysis. As the heating to continue, the second step of weight loss occurs (about 20 %) for $[\text{Eu}(\text{TTA})_4]\text{IM}^+\text{-Al}$ and (about 30 %) for $[\text{Eu}(\text{TTA})_4]\text{IM}^+\text{-Ti1}$ from 200 to 400°C , which is probably attributed by the unwashed europium tetrakis chelates, usually with the first decomposition of organic ingredients. It is the fastest stage of weight decline for both materials. Finally, the last weight loss beyond 420°C is attributed to the further decomposition of organic ingredients, which has almost the same mass loss (11 %) for the two types of materials. In comparison with the two types of materials, $[\text{Ln}(\text{L})_4]\text{IM}^+\text{-Al}$ presents better thermal stability than $[\text{Eu}(\text{TTA})_4]\text{IM}^+\text{-Ti1}$, presumably for the destruction of titanyl network.

The excitation spectra of Eu^{3+} hybrid soft xerogel materials $[\text{Eu}(\text{TAA})_4]\text{IM}^+\text{-Al}$ and $[\text{Eu}(\text{TAA})_4]\text{IM}^+\text{-Ti}(1,2)$ are shown in Figure 3 (left) by monitored at 613 nm. $[\text{Eu}(\text{TAA})_4]\text{IM}^+\text{-Al}$ shows an apparent strong broad band ranging from 250 to 450 nm, which is mainly originated from the absorption of TTA and charge transfer of Eu-O . While the sharp excitation in visible region is very weak for the f-f transition of Eu^{3+} , only 465 nm for ${}^7\text{F}_0 \rightarrow {}^5\text{D}_2$ transition can be observed. This illustrates that the energy transfer from TTA and Eu^{3+} can occur effectively in Al-O xerogel matrices. As for the excitation spectra data of $[\text{Eu}(\text{TAA})_4]\text{IM}^+\text{-Ti}(1,2)$, the broad band for europium complex at 300 ~ 400 nm becomes much weaker than that of $[\text{Eu}(\text{TAA})_4]\text{IM}^+\text{-Al}$ and instead a strong excitation band ranged in 400-450 nm (maximum 415 nm) in visible region appear, which may be derived from the IM^+ modified titania and needs to be studied deeply. Besides, the apparent sharp emission at 470 nm for ${}^7\text{F}_0 \rightarrow {}^5\text{D}_2$ transition of Eu^{3+} can be checked, much higher than that of $[\text{Eu}(\text{TAA})_4]\text{IM}^+\text{-Al}$. In titania xerogel system, the luminescent performance of europium complexes is not favorable as in alumina system, but the modified titania host will play a role for the luminescence of Eu^{3+} ion. The above predict can be verified in the corresponding emission spectra (Figure 3, right). Both alumina and titania xerogels all show the red luminescence of Eu^{3+} in spite of the different excitation (for alumina, 342 nm for $[\text{Eu}(\text{TAA})_4]$; for titania 411 nm for $\text{IM}^+\text{-Ti}$). As shown in Figure 3b, five emission bands assigned to the transitions ${}^5\text{D}_0 \rightarrow {}^7\text{F}_J$ ($J = 0-4$) for Eu^{3+} are at 577, 589, 613, 650, and 700 nm, respectively, in which ${}^5\text{D}_0 \rightarrow {}^7\text{F}_2$ transition at 613 nm is dominated with maximum intensity. Additionally, both $[\text{Eu}(\text{TAA})_4]\text{IM}^+\text{-Ti1}$ and $[\text{Eu}(\text{TAA})_4]\text{IM}^+\text{-Ti2}$ possess the color coordinate in red region in spite of different ratio of $\text{Eu}:\text{Ti}$. Furthermore, we know that ${}^5\text{D}_0 \rightarrow {}^7\text{F}_2$ transition is the typical electric dipole transition and strongly varies with the local symmetry of Eu^{3+} , which is independent in the host material, and once the micro-chemical environment offer stronger effects to Eu^{3+} , the complexes will become more asymmetric and stronger electric dipole transitions.

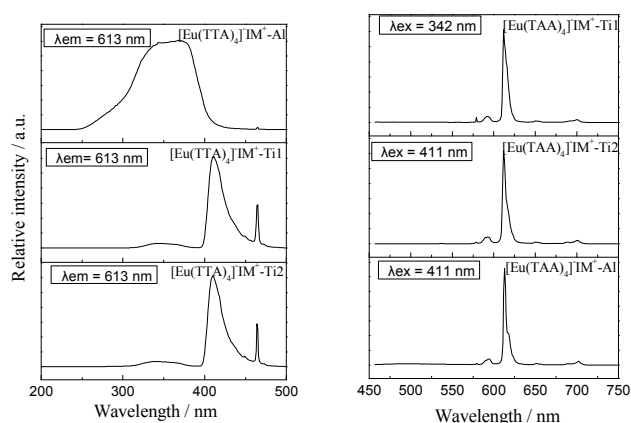


Figure 3 The excitation and emission spectra of Eu^{3+} hybrid soft xerogels $[\text{Eu}(\text{TAA})_4]\text{IM}^+\text{-Al}(\text{Ti1}, \text{Ti2})$.

Figure 4 (left) displays the excitation spectra of hybrid soft xerogels $[\text{Tb}(\text{TAA})_4]\text{IM}^+\text{-Al}$ and $[\text{Tb}(\text{TAA})_4]\text{IM}^+\text{-Ti}(1,2)$ by monitoring the characteristic emission of terbium ion at 545 nm, whose excitation spectra are consisted of a similar broad band from

250 to 400 nm and can be ascribed to the ligand absorption of TAA. This suggests the luminescence and energy transfer performance in both alumina and titania are similar. In addition, the excitation spectrum of $[\text{Tb}(\text{TAA})_4]\text{IM}^+\text{-Al}$ also shows the apparent f-f transition of Tb^{3+} in long-wavelength region, 351 nm (${}^7\text{F}_6 \rightarrow {}^5\text{G}_2$), 360 nm (${}^7\text{F}_6 \rightarrow {}^5\text{D}_2$), 372 nm (${}^7\text{F}_6 \rightarrow {}^5\text{G}_6$), and 380 nm (${}^7\text{F}_6 \rightarrow {}^5\text{D}_3$), respectively. But for $[\text{Tb}(\text{TAA})_4]\text{IM}^+\text{-Ti}(1,2)$, the excitation bands in long-wavelength region possess high baseline and poor shape, which may be related to the host absorption of $\text{IM}^+\text{-Ti}$. Figure 4 (right) shows the emission spectra of terbium hybrid xerogels. There are almost same positions of the emission bands for the three hybrid materials. Four apparent emission peaks can be observed at around 487, 545, 587, 621 nm, corresponding to the Tb^{3+} 's transitions from the ${}^5\text{D}_4$ excited state to the different J levels of the ground state ${}^5\text{D}_4 \rightarrow {}^7\text{F}_J$ ($J = 6, 5, 4, 3$). Comparing the emission spectra of $[\text{Tb}(\text{TAA})_4]\text{IM}^+\text{-Ti}(1,2)$ with different molar ratio of Tb^{3+} and titania, no significant change is found.

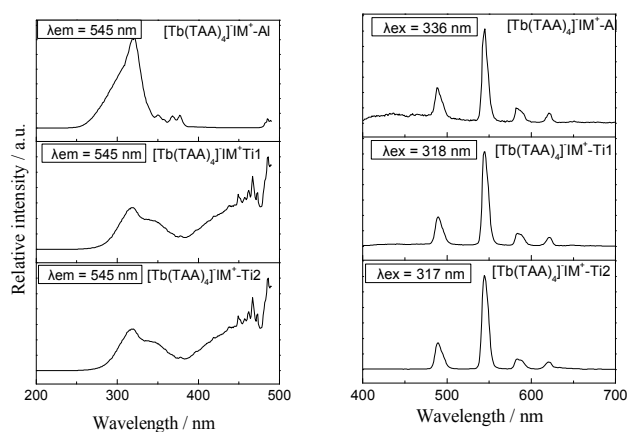


Figure 4 The excitation and emission spectra of Tb^{3+} hybrid soft xerogels $[\text{Tb}(\text{TAA})_4]\text{IM}^+\text{-Al}(\text{Ti1}, \text{Ti2})$.

Figure 5 shows the excitation and emission spectra of $[\text{Sm}(\text{TAA})_4]\text{IM}^+\text{-Al}$ and $[\text{Sm}(\text{TAA})_4]\text{IM}^+\text{-Ti}(1,2)$, respectively. For excitation spectra of them collected at the emission wavelength of 645 nm, the different band position can be checked. For $[\text{Sm}(\text{TAA})_4]\text{IM}^+\text{-Al}$ hybrids, its excitation spectrum shows an apparent strong broad band ranging from 250 to 450 nm, similar to $[\text{Sm}(\text{TAA})_4]\text{IM}^+\text{-Al}$ system, corresponding to the absorption of TTA and charge transfer of Sm-O . No apparent f-f transition of Eu^{3+} can be observed for its weak intensity. So the energy transfer from TTA and Sm^{3+} can be predicted to effectively take place in Al-O xerogel matrices. For the excitation spectra of $[\text{Sm}(\text{TAA})_4]\text{IM}^+\text{-Ti}(1,2)$, a broad band appears across 250- 400 nm with a maximum at around 348 nm, relevant to the charge transfer state Sm-O . Besides one apparent absorption band in the range of visible region 400 - 500 nm occur, it ascribed to the host absorption of IM^+ functionalized Ti-O network. Comparing the excitation spectra of $[\text{Sm}(\text{TAA})_4]\text{IM}^+\text{-Ti}(1,2)$ hybrids, it can be found that the different molar ratio of Sm^{3+} and titania host has influence on the relative excitation intensity ratio of Sm-O charge transfer and $\text{IM}^+\text{-Ti}$ host. Figure 5(right) shows the analogous predominant characteristic emission peak of Sm^{3+} for these hybrid xerogel materials, which is centered at ~565, ~600, ~645 nm and 722 ~nm assigned to ${}^4\text{G}_{5/2} \rightarrow {}^6\text{H}_{5/2}$, ${}^4\text{G}_{5/2} \rightarrow {}^6\text{H}_{7/2}$,

${}^4G_{5/2} \rightarrow {}^6H_{9/2}$, and ${}^4G_{5/2} \rightarrow {}^6H_{11/2}$, respectively. For $[\text{Sm}(\text{TAA})_4]\text{IM}^+-\text{Al}$ hybrids, its emission band (${}^4G_{5/2} \rightarrow {}^6H_{9/2}$ transition) at 645 nm possesses the highest intensity. While for $[\text{Sm}(\text{TAA})_4]\text{IM}^+-\text{Ti}(1,2)$ hybrids, two emission bands have the strongest intensity, 600 and 645 nm corresponding to ${}^4G_{5/2} \rightarrow {}^6H_{7/2}$ and ${}^4G_{5/2} \rightarrow {}^6H_{9/2}$ transitions. Simultaneously, a broad band of the emission spectra emerges across 380-500 nm in the range of blue-violet light, which is due to the intrinsic blue emission in alumina or titania host materials. Moreover, for $[\text{Sm}(\text{TAA})_4]\text{IM}^+-\text{Ti}2$ hybrids, the selective excitation with three different wavelengths (320, 349, 380 nm) all realized the white luminescence output, whose spectra are shown in Figure 6. The white luminescence can be integrated by adjusting the emission of both $[\text{Sm}(\text{TAA})_4]$ and IM^+-Ti host.

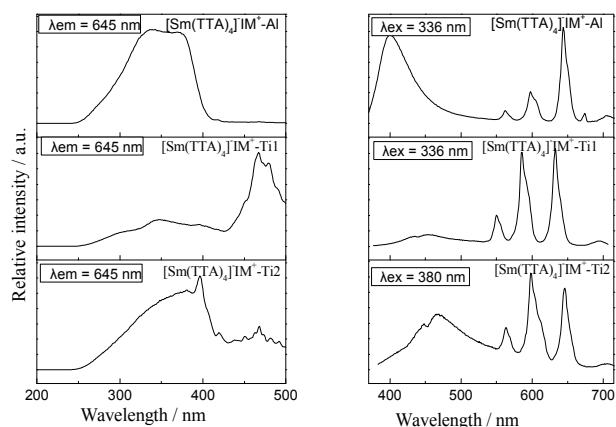


Figure 5 The excitation and emission spectra of Sm^{3+} hybrid soft xerogels $[\text{Sm}(\text{TAA})_4]\text{IM}^+-\text{Al}(\text{Ti}1, \text{Ti}2)$.

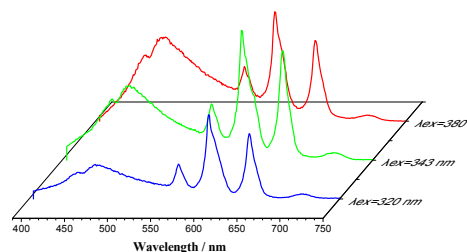


Figure 6 The emission spectra of Sm^{3+} hybrid soft xerogels $[\text{Sm}(\text{TAA})_4]\text{IM}^+-\text{Ti}2$ showing white luminescence

All the europium hybrid soft xerogels show the red emission, whose luminescent color can not be changed. While for europium hybrid soft xerogels, the luminescence color can be changed to the yellow zone from the green zone, according to the CIE chromaticity diagram (Figure 7(a)) of point 1 for $[\text{Tb}(\text{TAA})_4]\text{IM}^+-\text{Al}$; point 2 for $[\text{Tb}(\text{TAA})_4]\text{IM}^+-\text{Ti}1$ and point 3 for $[\text{Tb}(\text{TAA})_4]\text{IM}^+-\text{Ti}2$. For samarium hybrid soft xerogels, the luminescence color can be adjusted and the white luminescence integration can be realized. The corresponding CIE coordinates for the emission spectra of $[\text{Sm}(\text{TAA})_4]\text{IM}^+-\text{Ti}2$ in Figure 6 are determined as $x = 0.2990$, $y = 0.2946$, $x = 0.3323$, $y = 0.2951$ and $x = 0.3601$, $y = 0.31$, corresponded to monitored by 380, 343 and 320 nm respectively. They all are located in white region (point 2-4, Figure 7), which

provides more likely optimal conditions to achieve further study for the LED white lamps. The corresponding CIE coordinates for the emission spectra of $[\text{Sm}(\text{TAA})_4]\text{IM}^+-\text{Al}$ is determined as $x = 0.2406$, $y = 0.1601$, locating at the junction of the blue and pink as shown point 1, Figure 7(b). Theoretically, it will only move to pink region with increasing the amount of Sm^{3+} , and move to the blue region if reducing the amount of Sm^{3+} . Therefore, it is hard to simply adjust the amount of Sm^{3+} to stimulate white light. But for the same proportion of the doping equal amount of Sm^{3+} for $[\text{Sm}(\text{TAA})_4]\text{IM}^+-\text{Ti}(1,2)$ currently appearing in the color coordinates in point 5 (Figure 7(b)). It can be obtained white light by adjusting the quantity of Sm^{3+} . So a series of experiments are tried in order to further investigate the influence of different proportion of Sm^{3+} doped level on luminescence intensity and color of $[\text{Sm}(\text{TAA})_4]\text{IM}^+-\text{Ti}2$, it has been carried out to decrease the amount of doped Sm^{3+} to 2.5 % ($\text{Sm}:\text{Ti} = 1:40$).

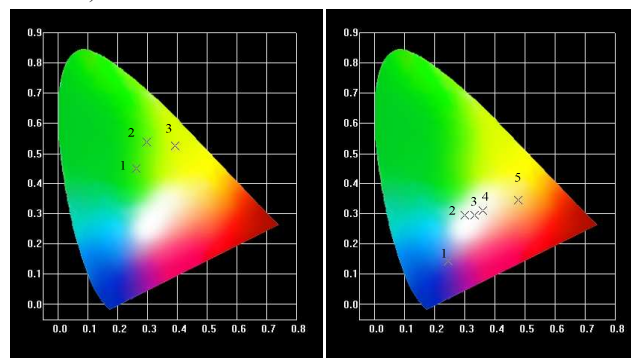


Figure 7 The color coordinate results of hybrid soft xerogels, (a) $[\text{Tb}(\text{TAA})_4]\text{IM}^+-\text{Al}(\text{Ti}1, \text{Ti}2)$ and (b) $[\text{Sm}(\text{TAA})_4]\text{IM}^+-\text{Al}(\text{Ti}1, \text{Ti}2)$.

Conclusion

In summary, luminescent hybrid materials $[\text{Ln}(\text{L})_4]\text{IM}^+-\text{Al}/\text{Ti}$ ($\text{Ln} = \text{Eu}, \text{Sm}$, $\text{L} = \text{TTA}$; $\text{Ln} = \text{Tb}$, $\text{L} = \text{TAA}$) have been synthesized via an ionic-bridge connecting lanthanide beta-diketonates with the matrix (Al-O or Ti-O networks) through sol-gel processes. Especially, the white-light emission can be integrated by regulating the ratio of Sm^{3+} complex and titania host through a broadband excitation. The results provide useful data to develop novel optical hybrid materials for optimizing the current technology of LED using a moderate and controllable technology.

Acknowledgements

This work is supported by the National Natural Science Foundation of China (20971100, 91122003) and Developing Science Funds of Tongji University.

Notes and references

^a Department of Chemistry, Tongji University, Shanghai, 200092, China. E-mail: byan@tongji.edu.cn; Fax: +86-21-65982287; Tel: +86-21-65984663

[†] Electronic Supplementary Information (ESI) available: [details of any supplementary information available should be included here]. See DOI: 10.1039/b000000x/

1 (a) Danielson, M. Devenney, D. M. Giaquinta, J. H. Golden, R. C. Haushalter, E. W. McFarland, D. M. Poojary, C. M. Reaves, W. H. Weinberg and X. D. Wu, *Science*, 1998, **279**, 837; (b) C. R. Ronda, T. Justel, H. Nikol, *J. Alloys Compds.*, 1998, **275**, 669; (c) H. Q. Wang, M.

- Batentschuk, A. Osvet, L. Pinna and C. J. Brabec, *Adv. Mater.*, 2011, **23**, 2675.
- 2 (a) E. Nakazawa, *J. Chem. Phys.*, 1967, **47**, 3211; (b) W. L. Wang, Q. K. Shang, W. Zheng, H. Yu, X. J. Feng, Z. D. Wang, Y. B. Zhang and G. Q. Li, *J. Phys. Chem. C*, 2010, **114**, 13663.
- 3 (a) L. H. Slooff, A. van Blaaderen, A. Polman, G. A. Hebbink, S. I. Klink, F. C. J. M. Van Veggel, D. N. Reinhoudt and J. W. Hofstra, *J. Appl. Phys.*, 2002, **91**, 3955; (b) D. J. Richardson, J. Nilsson and W. A. Clarkson, *J. Opt. Soc. Am. B-Opt. Phys.*, 2010, **27**, B63; (c) S. Tanabe, *Compt. Rend. Chim.*, 2002, **5**, 815.
- 4 (a) O. L. Malta and F. R. G. E. Silva, *Spectrochim. Acta a-Mol. Biomol. Spectros.*, 1998, **54**, 1593; (b) E. R. Souza, I. G. N. Silva, E. E. S. Teotonio, M. C. F. C. Felinto and H. F. Brito, *J. Lumin.*, 2010, **130**, 283; (c) X. J. Sun, W. X. Li, W. J. Chai, T. Ren and X. Y. Shi, *J. Fluores.*, 2010, **2**, 453.
- 5 (a) J. P. Sutter, M. L. Kahn, S. Golhen, L. Ouahab and O. Kahn, *Chem. Euro. J.*, 1998, **4**, 571; (b) K. C. Teixeira, G. F. Moreira, W. G. Quirino, C. Legnani, R. A. Silva, M. Cremona, H. F. Brito and C. A. Achete, *J. Therm. Anal. Cal.*, 2011, **106**, 587; (c) H. Tsukube and S. Shinoda, *Chem. Rev.*, 2002, **102**, 2389; (d) A. G. Trambitas, T. K. Panda, J. Jenter, P. W. Roesky, C. Daniliuc, C. G. Hrib, P. G. Jones and M. Tamm, *Inorg. Chem.*, 2010, **49**, 2435.
- 6 (a) J. Zhou, Y. Sun, X. X. Du, L. Q. Xiong, H. Hu and F. Y. Li, *Biomaterials*, 2010, **31**, 3287; (b) M. A. Katkova and M. N. Bochkarev, *Dalton Trans.*, 2010, **39**, 6599; (c) C. C. Mi.; J. P. Zhang, H. Y. Gao, X. L. Wu, M. Wang, Y. F. Wu, Y. Q. Di, Z. R. Xu, C. B. Mao and S. K. Xu, *Nanoscale*, 2010, **2**, 1141.
- 7 (a) J. Kulesza, B. S. Banos and S. Alves, *Coord. Chem. Rev.*, 2013, **257**, 2192; (b) J. Pyun and K. Matyjaszewski, *Chem. Mater.* 2001, **13**, 3436; (c) M. Vallet-Regi, M. Colilla and B. Gonzalez, *Chem. Soc. Rev.*, 2011, **40**, 596.
- 8 (a) J. E. C. da Silva, G. F. de Sa and P. A. Santa-Cruz, *J. Alloys Compds.*, 2002, **344**, 260; (b) H. Luo, J. K. Kim, E. F. Schubert, J. Cho, C. Sone and Y. Park, *Appl. Phys. Lett.*, 2005, **86**, 062104.
- 9 (a) W. S. Miao and T. H. Chan, *Acc. Chem. Res.*, 2006, **39**, 897; (b) H. Olivier-Bourbigou and L. Magna, *J. Mol. Catal. A-Chem.*, 2002, **182**, 419.
- 10 (a) J. P. Hallett and T. Welton, *Chem. Rev.*, 2011, **111**, 3508; (b) R. N. Das and K. Roy, *Mol. Divers.* 2013, **17**, 151; (c) R. N. Das and K. Roy, *Toxic. Res.*, 2012, **1**, 186.
- 11 (a) A. P. Abbott, G. Capper, D. L. Davies and R. Rasheed, *Inorg. Chem.*, 2004, **43**, 3447; (b) Y. Feng, H. R. Li, Q. Y. Gan, Y. G. Wang, B. Y. Liu and H. J. Zhang, *J. Mater. Chem.*, 2010, **20**, 972.
- [12] (a) P. Nockemann, B. Thijs, S. Pittois, J. Thoen, C. Glorieux, K. Van Hecke, L. Van Meervelt, B. Kirchner and K. Binnemans, *J. Phys. Chem. B*, 2006, **110**, 20978; (b) K. C. Lethesh, K. Van Hecke, L. Van Meervelt, P. Nockemann, B. Kirchner, S. Zahn, T. N. Parac-Vogt, W. Dehaen and K. Binnemans, *J. Phys. Chem. B*, 2011, **115**, 8424.
- 13 Q. P. Li, B. Yan, *Dalton Trans.*, 2012, **41**, 8567.
- 14 (a) G. Lee, *Chem. Commun.*, 2006, 1049; (b) J. C. MacDonald, P. C. Dorrestein and M. M. Pilley, *Cryst. Growth Des.*, 2001, **1**, 29.
- 15 (a) L. D. Carlos, R. A. S. Ferreira, V. D. Bermudez and S. J. L. Ribeiro, *Adv. Mater.* 2009, **21**, 509; (b) K. Binnemans, *Chem. Rev.*, 2009, **109**, 4283; (c) B. Yan, *RSC Adv.*, 2012, **2**, 9304; (d) J. Feng and H. J. Zhang, *Chem. Soc. Rev.*, 2013, **42**, 387.
- 16 (a) P. Nockemann, E. Beurer, K. Driesen, R. Van Deun, K. Van Hecke, L. Van Meervelt and K. Binnemans, *Chem. Commun.* 2005, **34**, 4354; (b) K. Lunstroot, K. Driesen, P. Nockemann, C. Gorller-Walrand, K. Binnemans, S. Bellayer, J. Le Bideau and A. Vioux, *Chem. Mater.*, 2006, **18**, 5711; (c) K. Lunstroot, P. Nockemann, K. Van Hecke, L. Van Meervelt, C. Gorller-Walrand, K. Binnemans and K. Driesen, *Inorg. Chem.*, 2009, **48**, 3018; (d) K. Lunstroot, K. Driesen, P. Nockemann, K. Van Hecke, L. Van Meervelet, C. Gorller-Warrand, K. Binnemanoux, S. Bellayer, L. Viau, J. Le Bideau and A. Vioux, *Dalton Trans.*, 2009, **38**, 298.
- 17 E. Gomez, B. Gonzalez, A. Dominguez, E. Tojo and J. Tojo, *J. Chem. Eng. Data*, 2006, **51**, 696.
- 18 L. P. Hou, Y. B. Su, Y. Yang and Y. P. Gao, *Synthesis, J. Appl. Polym. Sci.*, 2012, **123**, 472.
- 19 (a) L. Guo, L. S. Fu, R. A. S. Ferreira, L. D. Carlos, Q. P. Li and B. Yan, *J. Mater. Chem.*, 2011, **21**, 15600; (b) H. R. Li, P. Liu, H. F. Shao, Y. G. Wang, Y. X. Zheng, Z. Sun and Y. H. Chen, *J. Mater. Chem.*, 2009, **19**, 5533.
- 20 A. Islam, E. S. Chan, Y. H. Taufiq-Yap, S. H. Teo and M. A. Hoque, *Ceram. Inter.*, 2014, **40**, 3779.